Giant Magnetoresistive Sensors for Biological Applications

Jonathan Lee
Physics, University of Central Florida

NNIN REU Site: Nanofabrication Center, University of Minnesota-Twin Cities, Minneapolis, MN
NNIN REU Principal Investigator: Prof. Jian-Ping Wang, Electrical and Computer Engineering, University of Minnesota
NNIN REU Mentor: Todd Klein, Electrical and Computer Engineering, University of Minnesota
Contact: jondleee@knights.ucf.edu, jpwang@umn.edu, klei0349@umn.edu

Abstract:

Field-induced domain wall motion through the free magnetic layer of a spin valve nanowire has been observed both electrically and with Bitter Method on a scanning electron microscope. The giant magnetoresistance effect was used to determine the position of the domain wall. Change in depinning field strength due to the presence of magnetic nanoparticles (MNPs) was observed. This work served as preparation to extend to the sensing of biological molecules tagged with MNPs.

Introduction:

Some diseases increase the concentration of certain proteins in the blood, while others release proteins that would otherwise not be present. Giant magnetoresistive (GMR) sensors have shown the ability to detect target proteins with high sensitivity using MNPs as tags [1]. The device is sensitive to the presence of the MNP stray field, which shields the free layer of the sensor from an externally applied field, requiring more field strength to coerce the free layer magnetization in regions with MNPs present. GMR devices have been observed to detect proteins with a limit of detection in the hundreds of MNPs (< 100 nm diameter), which may miss a very low concentration detection.

To increase detection resolution, investigations were performed in order to manipulate and study the usefulness of magnetic domain walls (DW), which are native to the free layer of sensors with larger detection areas. The advantages of using magnetic DWs in this study were that GMR measurements have shown the location of DWs in the free layer of a GMR nanowire [2], and DWs have been shown to attract MNPs [3]. A smaller, curved sensor area has been studied here and has shown the possibility for increasing resolution to tens of particles.

Experimental Procedure:

Fabrication. The substrate consisted of a silicon <100> wafer with 100 nm of silicon dioxide (SiO_2) coating. The GMR metal stack was placed using a Shamrock RF sputtering device, placing thicknesses Ta 30Å / IrMn 80Å / CoFe 25Å / Cu 40Å / CoFe 20Å / NiFe 55Å / Ta 50Å.

Sensor areas were designed to have curved shapes in order to easily place magnetic domain walls [4].

Devices were patterned using electron beam lithography with negative resist. The developed resist pattern shielded the sensors from ion-milling employed to remove surrounding metals. Removal of the patterned resist left only the devices on the substrate. Contacts were placed using electron beam lithography followed by an electron beam evaporated metal deposition of 800Å Cu.

Testing. A constant current of 10 μA was passed through a device and the voltage across the device measured to calculate device resistance. Data from each device was actively recorded using LabVIEW software reading from a Keithley 2400 SourceMeter during various external magnetic field conditions.

DW depinning strengths were observed multiple times for several nanowires in order to confirm repeatability. Nanowire depinning measurements for the forward and reverse directions were recorded. Domain walls were induced near the center of a device by applying and then removing a magnetic field as shown in Figure 1A. During this step, the free layer aligned to the external field, and, when the field was removed,

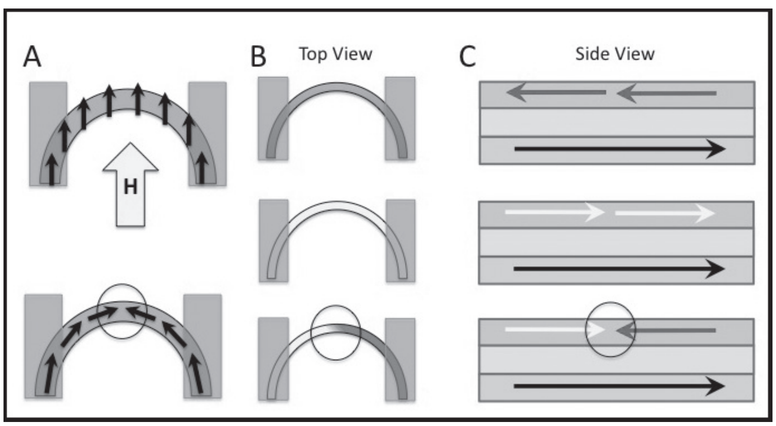

Figure 1: A) Device top view showing domain wall pinning schematic. B) and C) Top and side view of device in three resistance stages. White is parallel, and dark is antiparallel.

the magnetic direction of the free layer relaxed and aligned with the shape-anisotropic direction of the device — leaving a head-to-head domain wall near the middle of the sensing area. The nanowires were then exposed to a diluted solution of 35 nm superparamagnetic iron oxide particles and allowed to incubate for three hours before washing.

Results and Conclusions:

Resistance measurements before and after DW creation showed an intermediate state, approximately half way between the high and low states. DW depinning field strengths were measured from the central pinning site.

DW depinning field strength was measured by placing a DW near the center of a device using the previously stated method and monitoring resistance as the field was slowly increased from zero in a horizontal direction. DW pinning sites result from fabrication roughness at edges and defects in the wire (contaminant particles, layer unevenness, etc.). Depinning strengths were measured for 200 nm wide nanostripes with and without designed notches of 60 nm. The depinning strengths were ~ 50 Oe, noticeably higher than those with no obvious fabrication roughness < 40 Oe. Also, there were no observable secondary pinning sites for the sensors with notches.

MNP presence was verified using scanning electron microscopy (SEM) before depinning field strength measurements were retaken. By observing the field depinning strength of a device before and after particle application, one could see a shift in the field. A sensor with 8 MNPs on its sensing surface showed a depinning field strength increase of approximately 8 ± 2 Oe, see Figure 4. This is a promising result for progressing the diagnostic capability of GMR biosensors to include detection of target molecules with low concentrations.

Acknowledgements:

This work was funded by the National Science Foundation, the National Nanotechnology Infrastructure Network REU program, and the University of Minnesota. My sincerest gratitude to Dr. Jian-Ping Wang and his group for their guidance and support, with special thanks to Todd Klein, Angeline Klemm, and the UMN Nanofabrication Center staff.

References:

[1] Edelstein, R.L., C.R. Tamanaha, P.E. Sheehan, M.M. Miller, D.R. Baselt, L.J. Whitman, and R.J. Colton. 2000. Biosensors and Bioelectronics 14, 805-813.

[2] Boulle, O., G. Malinowski, and M. Klaui. 2011. Materials Science and Engineering R 72, 159-187.

[3] Vavassori, P. P., Metlushko, V. V., Ilic, B. B., Gobbi, M. M., Donolato, M. M., Cantoni, M. M., and Bertacco, R. R. (2008). Applied Physics Letters, vol. 93 (20), 203502.

[4] Saitoh, Eiji, Hideki Miyajima, Takehiro Yamaoka, and Gen Tatara. 2004. Nature 432, 203-206.

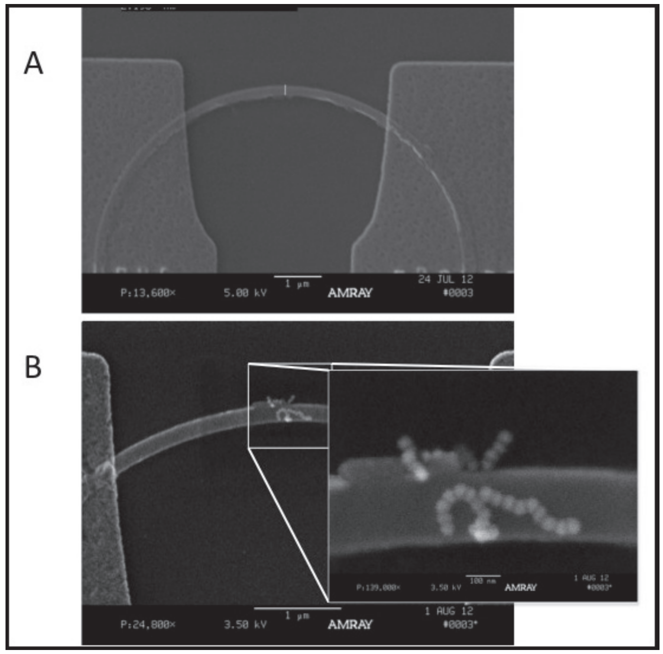

Figure 2: A) SEM image of device without MNPs. B) SEM image of device with MNPs.

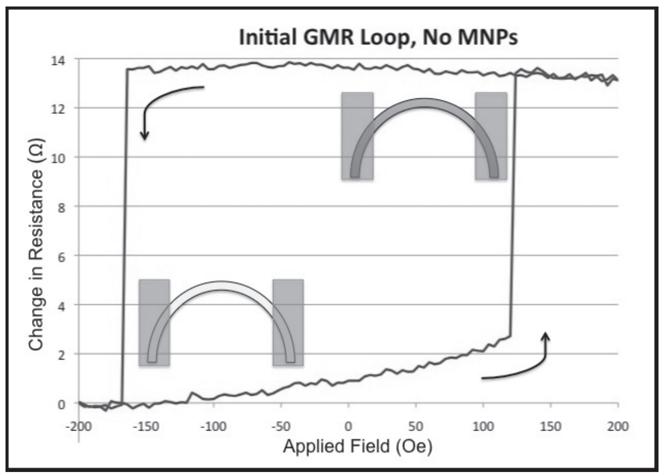

Figure 3: Graph showing the change in resistance by applied field.

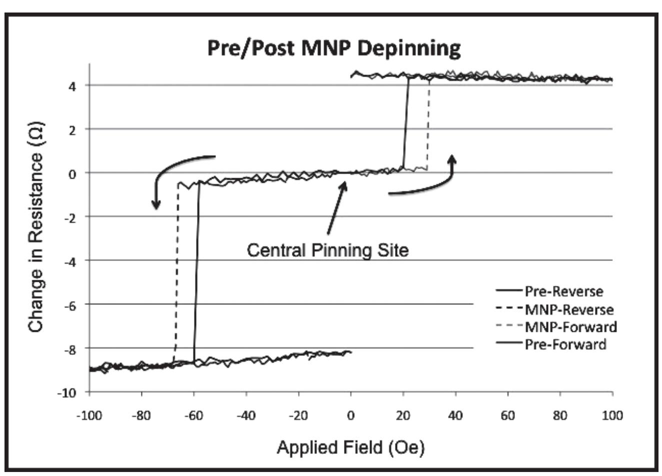

Figure 4: Graph showing the change in resistance from the central pinning site of a device both before (solid) and after (dashed) MNP placement.